Pseudospin polarized quantum transport in monolayer graphene

Leyla Majidi and Malek Zareyan[1]

[1]*Institute for Advanced Studies in Basic Sciences (IASBS), P. O. Box 45195-1159, Zanjan 45195, Iran*

Monolayer graphene with an energy gap presents a pseudospin symmetry broken ferromagnet with a perpendicular pseudomagnetization whose direction is switched by altering the type of doping between n and p. We demonstrate an electrical current switching effect in pseudospin version of a spin valve in which two pseudoferromagnetic regions are contacted through a normal graphene region. The proposed structure exhibits a pseudomagnetoresistance, defined as the relative difference of resistances of parallel and antiparallel alignments of the pseudomagnetizations, which can be tuned to unity. This perfect pseudomagnetic switching is found to show a strong robustness with respect to increasing of the contact length, the effect which we explain in terms of an unusually long range penetration of an equilibrium pseudospin polarization into the normal region by proximity to a pseudoferromagnet. Our results reveals the potential of gapped graphene for realization of pseudospin-based nanoelectronics.

PACS numbers: 73.23.-b, 72.25.-b, 72.80.Vp, 85.75.-d

I. INTRODUCTION

Graphene, the two dimensional layer of the carbon atoms with honeycomb lattice structure, has attracted a great deal of attention as a new promising material for nanoelectronics, since its experimental realization a few years ago[1–3]. Most of the peculiar properties of graphene is the result of its massless Dirac spectrum of the low-lying electron-hole excitations, which in addition to the regular spin appear to come endowed with the two quantum degrees of freedom, the so called pseudospin and valley. The pseudospin represents the sublattice degree of freedom of the graphene's honeycomb structure, and the valley defines the corresponding degree of freedom in the reciprocal lattice[2,6–9]. The effect of these additional quantum numbers has already been exploited by anomalous features of several quantum transport phenomena in graphene, including quantum Hall effect[2–5], conductance quantization[10], Klein tunneling[11–13] and quantum shot noise[14–16].

Interestingly, the pseudospin and valley degrees of freedom in graphene have been proposed separately to be used for controlling the electronic devices in the same way as the electron spin is used in spintronic and quantum computing. Rycerz *et al.*[17–19] demonstrated an electrostatically controlled valley filter effect in graphene nanoribbons with zigzag edge which can be used for realizing valley valve structures in valleytronics (valley-based electronics) applications. On the other hand a pseudospin-based version of a spin valve has been proposed in bilayer graphene, where the pseudospin is determined by the relative amplitude of the wave function on the two layers[20]. A bilayer pseudospin valve consists of two connected neighboring regions whose pseudospin polarizations can be tuned by application of gate voltages[21].

In this paper, we study the possibility of realizing pseudospintronics in monolayer graphene within the scattering formalism. The possibility of an interaction driven spontaneous breaking of the pseudospin symmetry, which can lead to the realization of pseudomagnetic states in monolayer and bilayer graphene, has been studied recently[22]. Here, we demonstrate that the monolayer graphene with a gap in its electronic spectrum and an appropriate doping presents a pseudospin symmetry broken ferromagnet, with a finite pseudospin magnetization oriented vertically to the graphene plane. The magnitude of the pseudomagnetization (PM) depends on the chemical potential and its direction is switched by changing the type of doping (electron n or hole p).

Based on the above observation, we propose a nonmagnetic pseudospin valve which consists of two pseudoferromagnetic (PF) regions separated by a non-pseudomagnetizaed normal (N) graphene of length L (shown schematically in Fig. 1b). The PM direction in each region can be tuned independently by means of electrical gates, which allows for switching between parallel and antiparallel configurations. We find that the proposed PF/N/PF spin valve exhibits a relative difference of the electrical resistance in the two parallel and antiparallel states of the pseudomagnetizations, which can be remarkably large in analogy to the giant magnetoresistance (GMR) in magnetic multilayers[23]. When the chemical potential of the system is tuned to be close to the energy gap ($\mu \simeq \Delta$), the pseudospin valve effect can be perfect PMR takes the value 1 for appropriate choices of the length L. More importantly, we show that the perfect pseudospin valve effect can be reached even in higher chemical potentials $\mu \gg \Delta$ by applying an appropriate bias voltage. We further demonstrate the unusual proximity effect at pseudoferromagnet-normal junctions (PF/N, PF/N/PF). We find that an equilibrium pseudospin polarization is induced into the N region with a direction which is precessing around the axis normal to the PF/N interface, and an amplitude which decays slowly in the distances of few Fermi wave length λ_F from the interface. This is in clear contrast to the induced magnetization in ordinary ferromagnet-normal metal junctions, which decays exponentially within λ_F[24].

This paper is organized as follows. In Sec. II, we introduce pseudoferromagnets (PF) and use them to study the

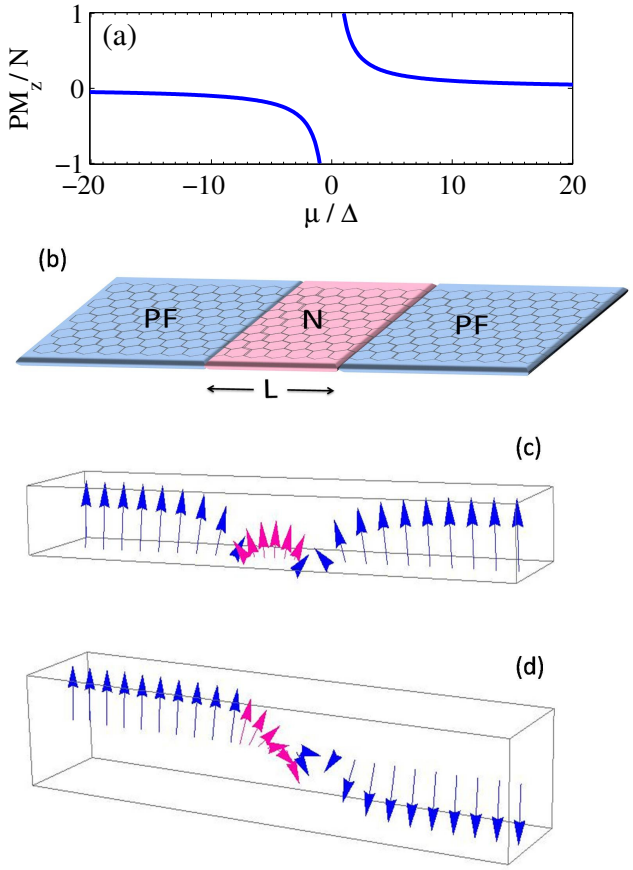

FIG. 1: (Color online) (a) Vertical pseudomagnetization per electron PM_z/N of the gapped graphene layer versus chemical potential μ (μ is scaled to the energy gap Δ). (b) Schematic illustration of the proposed pseudospin valve in monolayer graphene: The left and right regions are pseudoferromagnets (PF) and the intermediate region is a normal graphene (N) without a band gap. (c-d) Profile of pseudomagnetization vector $\boldsymbol{PM}$ inside the two PFs (blue) and the N region of length $L = \lambda_F$ (pink) for two configurations of (c) parallel and (d) anti-parallel, when $\mu \simeq \Delta$.

pseudospin valve effect in monolayer graphene PF/N/PF junction. Sec. III is devoted to the investigation of the proximity effect in graphene PF/N junctions. Finally, we present the conclusion in Sec. IV.

II. PSEUDOSPIN VALVE

The pseudospin valve structure we study is shown schematically in Fig. 1b. It consists of two PF regions with tunable direction of PM which are connected through a normal (non-pseudomagnetized) layer of length L. Such a structure can be realized in a graphene sheet with a sizable gap in its electronic band structure. There are several methods to open an energy gap in the band structure of graphene. A scenario is placing graphene on top of an appropriate substrate which breaks the graphene sublattice symmetry and generates a Dirac mass for charge carriers. The band gap opening is observed in epitaxially grown graphene on a SiC substrate[25,26] and a hexagonal boron nitride crystal[27], and also on metallic surfaces with a boron nitride buffer layer[28]. The energy band gap engineering can be also achieved through doping the graphene with several molecules such as CrO_3, NH_3, H_2O[29,30]. A gapped graphene with a chemical potential μ close to its energy gap Δ acquires a PM of sizable magnitude and an orientation which switches with changing the sign of the chemical potential (see Fig. 1a). A highly doped gapped graphene has a vanishingly small PM and behaves as a non-pseudomagnetized (normal) graphene.

To study quantum transport in the pseudospin valve structure within the scattering formalism, we first construct the quasiparticle wave functions that participate in the scattering processes. We adopt Dirac equation of the form

$$H\psi = (\varepsilon + \mu)\psi, \tag{1}$$

where in the presence of an energy gap $H = v_F(\boldsymbol{\sigma}.\boldsymbol{p}) + \Delta\sigma_z$ is the two-dimensional Dirac Hamiltonian with $\boldsymbol{p} = -i\hbar\boldsymbol{\nabla}$ the momentum operator in the x-y plane ($v_F = 10^6$ m/s represents the Fermi velocity) and $\boldsymbol{\sigma} = (\sigma_x, \sigma_y, \sigma_z)$ the vector of the Pauli matrices operating in the space of two sublattices of the honeycomb lattice[31,32]. The two-dimensional spinor has the form $\psi = (\psi_A, \psi_B)$, where the two components give the amplitude of the wave function on the two sublattices and ε is the quasiparticle energy.

For a uniform gapped graphene region the solutions of the Dirac equation Eq. (1) are two states of the form

$$\psi_c^{e\pm} = e^{\pm ik_c x} e^{iqy} \begin{pmatrix} e^{\mp i\alpha_c/2} \\ \pm e^{-\phi_c} e^{\pm i\alpha_c/2} \end{pmatrix}, \tag{2}$$

for conduction band electrons of n-doped graphene and

$$\psi_v^{e\pm} = e^{\mp ik_v x} e^{iqy} \begin{pmatrix} e^{\pm i\alpha_v/2} \\ \pm e^{\phi_v} e^{\mp i\alpha_v/2} \end{pmatrix}, \tag{3}$$

for valance-band electrons of p-doped graphene, at a given energy ε and transverse wave vector q with the energy-momentum relation $\varepsilon_{c,v} = \pm[-\mu + \sqrt{\Delta^2 + (\hbar v|\boldsymbol{k}_{c,v}|)^2}]$. Here $\alpha_{c,v} = \arcsin(\hbar vq/\sqrt{(\varepsilon \pm \mu)^2 - \Delta^2})$ is the angle of propagation of electron which has longitudinal wave vector $k_{c,v} = (\hbar v_F)^{-1}\sqrt{(\varepsilon \pm \mu)^2 - \Delta^2}\cos\alpha$ and $\phi_{c,v} = arcsinh(\Delta/\sqrt{(\varepsilon \pm \mu)^2 - \Delta^2})$. The two propagation directions of electron along the x axis are denoted by $\pm$ in $\psi_{c,v}^{e\pm}$.

The pseudospin of such states for conduction (valance) band electrons of n- (p-)doped graphene is obtained as

$$< \boldsymbol{\sigma}(\boldsymbol{k}) >_{\psi_{c,v}} = \sqrt{1 - (\frac{\Delta}{\varepsilon \pm \mu})^2}\ \hat{\boldsymbol{k}}_{c,v} + \frac{\Delta}{\varepsilon \pm \mu}\ \hat{\boldsymbol{k}}_{\perp}, \tag{4}$$

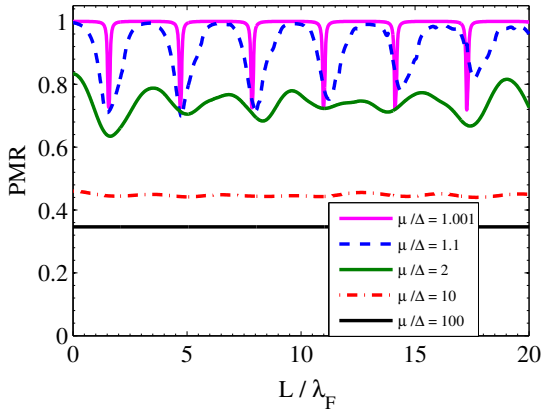

FIG. 2: (Color online) Pseudomagnetoresistance (PMR) of the pseudospin valve versus the length of the N region (L/λ_F) for different values of μ/Δ.

where $\hat{\boldsymbol{k}}_\perp$ is the unit vector normal to the electronic wave vector $\boldsymbol{k}_{c,v}$.

As can be seen from the above equation, the existence of a band gap makes the pseudospin to have a component perpendicular to the electronic momentum in the plane of the graphene sheet. The in-plane and out of plane components of the pseudospin depend on $(\varepsilon+\mu)/\Delta$, which can be tuned to unity to make the pseudospin vector to be oriented perpendicular to the sheet. Increasing $(\varepsilon+\mu)/\Delta$ leads to the decrease of the out of plane component such that it goes to zero when $\varepsilon+\mu \gg \Delta$.

The total PM of the gapped graphene is calculated by summing the expression (4) over all the wave vectors $\boldsymbol{k}=(k,q)$,

$$\boldsymbol{PM}_{n,p} = \sum_{\boldsymbol{k}} < \boldsymbol{\sigma}(\boldsymbol{k}) >_{\psi_{c,v}}, \tag{5}$$

from which we find that PM only has an out of plane component which depends on $(\varepsilon+\mu)/\Delta$. Fig. 1a shows the behavior of the out of plane component of PM per electron PM_z/N as a function of μ/Δ at zero temperature ($T=0$). It is seen that for $\mu \simeq \Delta$, PM_z/N takes its maximum value $PM_z/N=1$, while increasing μ/Δ leads to the decrease of PM_z such that it goes to zero for highly doped gapped graphene ($\mu \gg \Delta$). For a given value of $|\mu|$, the orientation of PM changes by changing the sign of μ/Δ. This implies that the PM vectors of gapped graphene regions with different type (n or p) of dopings are oriented antiparallel versus each other.

We note that the pseudospin polarization of a gapped graphene corresponds to a difference in the electronic charge densities of the two triangular sublattices, which in turn produces an in-plane electrical polarization of the density $\boldsymbol{P}_{n,p}=\sum_{\boldsymbol{k}}\boldsymbol{p}_{n,p}$. An electron with a wave vector $\boldsymbol{k}$ contributes a dipole moment which is calculated from the relation

$$\begin{aligned}\boldsymbol{p}_{n,p} &= \pm(1-|\frac{\psi_B}{\psi_A}|^{\pm 2}_{c,v})\ e\ \boldsymbol{a}_{AB} \\ &= \pm(1-e^{-2\phi_{c,v}})\ e\ \boldsymbol{a}_{AB},\end{aligned} \tag{6}$$

where $\boldsymbol{a}_{AB}$ is the lattice vector oriented from A to B site. We see that the electric dipole moments are oriented from A to B (B to A) sites for n- (p-)doped gapped graphene. This correspondence between PM vector and the density of the in-plane electrical polarization can be used for an experimental measuring of PM.

With the above found behavior of PM, the realization of the pseudospin valve of Fig. 1b seems quite feasible. The configuration of the pseudospin valve can be changed from parallel to antiparallel by fixing the type of doping of one region and changing the type of the doping in the other region. The size of the pseudospin valve effect is determined by the extent in which the conduction of the anti-parallel configuration is suppressed (similar to the spin valve effect). The pseudomagnetoresistance of a pseudospin valve is defined as

$$PMR = \frac{R_{AP}-R_P}{R_{AP}} = \frac{G_P-G_{AP}}{G_P}, \tag{7}$$

where $R_{P(AP)}$ is the resistance of the parallel (anti-parallel) configuration and $G_{P(AP)}$ is the corresponding conductances, which can be calculated from the Landauer formula[33]

$$G_{P(AP)} = g_0 \int |t_{P(AP)}|^2 \cos\alpha\ d\alpha, \tag{8}$$

where $T_{P(AP)}=|t_{P(AP)}|^2$ is the transmission probability of electrons through the pseudospin valve in parallel (anti-parallel) configuration and $g_0=4e^2/h$ is the quantum of conductance.

We have calculated the amplitudes of the transmission $t_{P(AP)}$ by matching the wave functions of three regions of the left PF, N region and the right PF (signed by 1,2, and 3, respectively) at the two interfaces, $x=0$ and $x=L$. The solutions of Eq. (1) in the three regions for parallel (P) and antiparallel (AP) configurations are as follow

$$\begin{aligned}\psi_1 &= \psi_c^{e+} + r\ \psi_c^{e-}, \\ \psi_2 &= a\ \psi_c^{\prime e+} + b\ \psi_c^{\prime e-}, \\ \psi_{3,P(AP)} &= t_{P(AP)}\ \psi_{c(v)}^{e+}.\end{aligned} \tag{9}$$

$\psi_{c(v)}^{(\prime)e\pm}$ are the wave functions of Dirac equation for incoming and outgoing electrons of n- (p-)doped graphene sheet with (without) a gap; r is the reflection coefficient in the left PF and a and b are the coefficients of the states $\psi_c^{\prime e\pm}$. Matching these solutions at the interfaces, we obtain the transmission amplitudes as

$$t_P = \frac{A\ e^{-ik_3 L}}{C+D+e^{i\alpha_3-\phi_3}\ (B+(e^{2ik_2L}-1)e^{-i\alpha_2})}, \tag{10}$$

$$t_{AP} = \frac{A\ e^{ik_3 L}}{e^{\phi_3}(B + e^{i\alpha_2}(1 - e^{2ik_2 L})) + C + De^{i\alpha_3}}, \quad (11)$$

where $A = 4\cos\alpha_1 \cos\alpha_2\ \ exp(i[\frac{\alpha_1+\alpha_3}{2} + \alpha_2 + k_2 L])$, $B = exp(i\alpha_1 + i\phi_1)\ [exp(2i\alpha_2) + exp(2ik_2 L)]$, $C = [1 - exp(2ik_2 L)]\ exp(i[\alpha_1 + \alpha_2] + \phi_1)$ and $D = 1 + exp(2i\alpha_2 + 2ik_2 L)$.

Finally from the calculated expressions of G_P and G_{AP} via Eq. (8) and using Eq. (7), we obtain PMR as a function of the chemical potential and the length of the N region. Fig. 2 shows dependence of PMR on $L/\lambda_F (\lambda_F = \hbar v_F/\mu)$ at $T = 0$ and zero bias voltage $V = 0$ and for different values of μ/Δ. We have taken $\mu_1 = \mu_2 = |\mu_3| = \mu$. We observe that the pseudospin valve effect can be perfect ($PMR = 1$) for $\mu \simeq \Delta$. For these values of μ, PMR shows an oscillatory behavior with L/λ_F, with an amplitude which takes the value 1 for some ranges of the length. We note that this perfect pseudospin valve effect of the monolayer graphene is more robust with respect to an increase of the length of the N region, as compared to the similar effect in a bilayer graphene pseudospin valve structure[20].

The amplitude of PMR decreases by increasing μ/Δ and tends to the constant value of $PMR = 1/3$ for a highly doped structure with $\mu \gg \Delta$. This residual PMR is the difference in the resistance of a n-p graphene structure with that of a uniformly (p or n) doped graphene with the same $|\mu|$, which is present even in the limit $PM \to 0$ of a non-pseudomagnetized structure.

We have found that the perfect pseudospin valve effect can be resumed by applying a bias voltage V of an appropriate amplitude to the valve. This is shown in Fig. 3a,b. In Fig. 3a, PMR is plotted versus L/λ_F for $\mu/\Delta = 2$ and different eV/Δ. As it is seen, by increasing eV from 0 the amplitude of PMR increases and the oscillatory behaviour is suppressed, such that PMR reaches the perfect constant value 1 when $eV = \Delta$. Fig. 3b shows plot of PMR as a function of eV/Δ for different values of L/λ_F, which shows that the pseudospin valve becomes perfect as $eV \to 1$, independent of the value of L/λ_F. Applying bias voltage is such that there is no band crossing for p-doped excitations ($eV \leq \mu - \Delta$). This is similar to the case of having PF regions with different chemical potentials, where $\mu_{n,p} = eV \pm \mu$ and $\mu_n \geq |\mu_p|$.

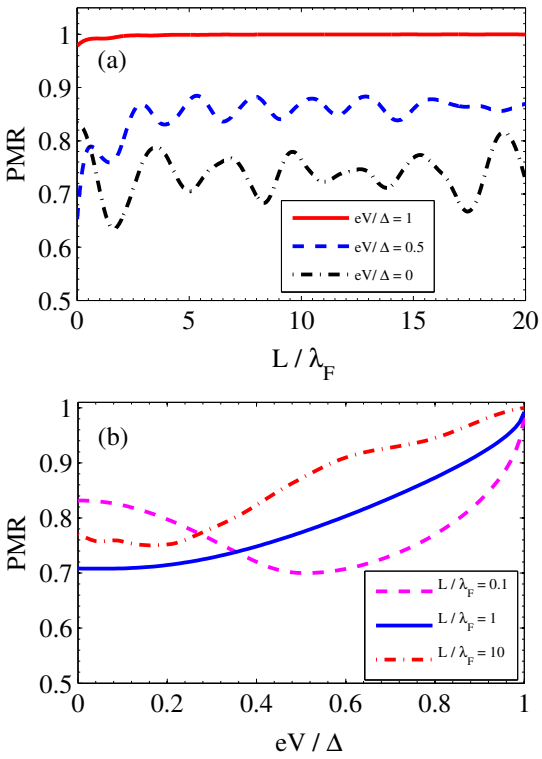

FIG. 3: (Color online)(a) Plot of PMR versus L/λ_F for three values of bias voltage $eV/\Delta = 0, 0.5, 1$ (b) and the behavior of PMR versus eV/Δ for three values of L/λ_F, when $\mu = 2\ \Delta$.

III. PROXIMITY EFFECT IN PF/N JUNCTIONS

The above found strong robustness of the pseudospin valve effect with respect to increasing the length of N contact should arise from a strong pseudomagnetic coupling between the two graphene PF regions. This itself can be due to a long range penetration of pseudospin polarization into the N region by proximity to PF regions. To analyze this in detail, we study proximity effect in PF/N, PF/N/PF junctions. We start with a single PF/N junction in a graphene sheet in the x-y plane, where the region $x < 0$ (PF region) has a uniform PM oriented vertically to the sheet and the region $x > 0$ (N region) is in the normal state. We calculate PM in PF and N regions using Eq. (5), and by considering the contribution of the pseudospin of all incident electrons from left and right regions that are scattered from the junction. The total pseudomagnetization vector $\boldsymbol{PM}$ will be the sum of PM vectors contributed from electrons incident from the left and the right regions:

$$\frac{\boldsymbol{PM}_j}{N_j} = \frac{1}{2}\{\frac{\boldsymbol{PM}_j^l}{N_j^l} + \frac{\boldsymbol{PM}_j^r}{N_j^r}\},$$
$$\boldsymbol{PM}_j^{l(r)} = \sum_{\boldsymbol{k}} < \boldsymbol{\sigma}(\boldsymbol{k}) >_{\psi_{j,l(r)}}, \quad (12)$$
$$N_j^{l(r)} = \sum_{\boldsymbol{k}} \psi^*_{j,l(r)}\psi_{j,l(r)},$$

where j denotes the PF(N) region.

The resulting profile of $\boldsymbol{PM}$ across the PF/N junction is demonstrated in Fig. 4 for $\mu \simeq \Delta$. As it is seen, a nonzero $\boldsymbol{PM}$ is induced in N region ($\Delta = 0$) which rotates around the normal to the junction (x axis) with x. The perpendicular component PM_z oscillates as a function of x with a period of order λ_F, and shows only a weak decay in the scale of λ_F. While the in-plane com-

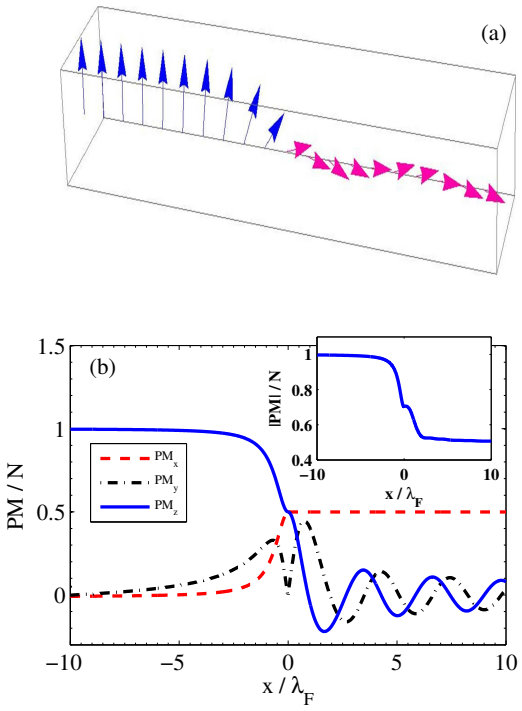

FIG. 4: (Color online) PM of the PF/N junction when $\mu \simeq \Delta$: The profile of $\boldsymbol{PM}$ in PF (blue) and N regions (pink) (a) and the position dependence of the $\boldsymbol{PM}$ components (b). The inset of Fig. 4b shows the magnitude of $\boldsymbol{PM}$.

ponents $PM_{x,y}$ vanish inside the PF regions, they are produced at the PF/N interface and are penetrated into the N region. This is originated from the difference between the pseudospin of electrons coming from PF side (Eq. (4)) and that of electrons coming from N side (Eq. (4) with $\Delta = 0$), which results in a nonvanishing averaged over momentum directions pseudospin polarization. The y component PM_y shows an oscillatory behaviour with x similar to PM_z. Interestingly, PM_x is uniform inside N, which considering the decay of the other two components, implies that $\boldsymbol{PM}$ at the points in N far from the junction is uniform and oriented perpendicular (along x axis) to the $\boldsymbol{PM}$ in the connected PF. This unusual proximity effect can be explained in terms of reflectionless Klein transmission of electrons which incident normally to PF/N interface[11–13]. We note to the unusually long range penetration of the proximity induced PM inside the N region, which is in contrast to the ferromagnet/normal metal junction (FN), in which the induced magnetization decays over short interatomic distances.

The above analysis of the proximity effect in PF/N junction can be extended to the pseudospin valve geometry of Fig. 1b. The profile of $\boldsymbol{PM}$ orientation in different regions of the PF/N/PF junction is indicated in Fig. 1 for parallel (c) and antiparallel (d) cases when $L = \lambda_F$ and $\mu \simeq \Delta$. $\boldsymbol{PM}$ is perpendicular to the x-axis and undergoes rotation across the N contact in a way that in P

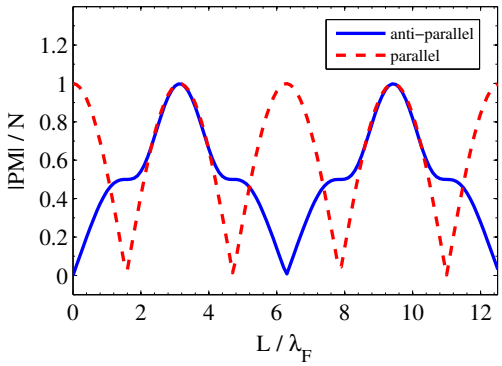

FIG. 5: (Color online) Plot of PM dependance on the length of the N region L/λ_F for PF/N/PF junctions, where $\mu \simeq \Delta$.

and AP cases PM_y and PM_z, respectively, shows change of signs at the middle of N region ($x = L/2$).

Furthermore, we obtain that the magnitude of $\boldsymbol{PM}$ inside the N region is constant with x for both of parallel and anti-parallel configurations. Dependence of the magnitude of $\boldsymbol{PM}$ on the length of the N region L and for $\mu/\Delta \simeq 1$, is shown in Fig .5 for both of parallel and anti-parallel configurations. We see that they have a periodic behavior with L. As is expected, in the limit $L \to 0$ pseudomagnetization of the parallel configuration goes to the constant value of a PF layer $|PM|/N = 1$, while it tends to zero for anti-parallel configuration (n-p junction).

IV. CONCLUSION

In conclusion, we have investigated realization of pseudospin polarized quantum transport in monolayer graphene with an energy gap in its Dirac spectrum. We have demonstrated that a gapped graphene is a pseudospin symmetry-broken state which exhibits a pseudomagnetization PM oriented normal to plane of the graphene. The magnitude of PM depends on the ratio of the chemical potential to the energy gap μ/Δ and its direction is switched by changing the type of doping between n and p. Based on this observation, we have proposed a pseudospin valve in which a non-pseudomagnetized normal region connects two pseudoferromagnetic (PF) regions, whose magnetization alignment can be controlled by altering the type of their doping. The suggested pseudospin valve exhibits a pseudomagnetoresistance PMR, defined as the relative difference of the resistances in parallel and antiparallel alignments, which for $\mu \simeq \Delta$ can be tuned to unity by appropriately adjusting the contact length L. We have shown that this perfect pseudomagnetic valve effect with $PMR = 1$ is preserved even for very large lengths $L \gg \lambda_F$. Although PMR decreases by increasing μ/Δ in the absence of a bias voltage, a perfect switching at large chemical potentials

can be resumed by applying an appropriate bias voltage.

In order to explain the robustness of the pseudospin valve effect with respect to increasing of the contact length, we have further studied the proximity effect in PF/N junctions. We have found that an equilibrium pseudospin polarization can be induced in the normal graphene over a very large length $L \gg \lambda_F$. The induced pseudomagnetization vector $\boldsymbol{PM}$ undergoes a damped spatial precession around the normal to the PF/N junction and tends to be uniform along the normal at the large distances $x \gg \lambda_F$ from the junction.

Acknowledgments

We thank A. G. Moghaddam for fruitful discussions. The authors gratefully acknowledge support by the Institute for Advanced Studies in Basic Sciences (IASBS) Research Council under grant No. G2009IASBS110.

[1] K. S. Novoselov, A. K. Geim, S. V. Morozov, D. Jiang, Y. Zhang, S. V. Dubonos, I. V. Grigorieva, and A. A. Firsov, Science **306**, 666 (2004).
[2] K. S. Novoselov, A. K. Geim, S. V. Morozov, D. Jiang, M. I. Katsnelson, I. V. Grigorieva, S. V. Dubonos, and A. A. Firsov, Nature **438**, 197 (2005).
[3] Y. Zhang, Y.- W. Tan, H. L. Stormer, and P. Kim, Nature **438**, 201 (2005).
[4] V. P. Gusynin and S. G. Sharapov, Phys. Rev. Lett. **95**, 146801 (2005).
[5] Xu Du, Ivan Skachko, Fabian Duerr, Adina Luican, and Eva Y. Andrei, Nature **462**, 192 (2009).
[6] P. R. Wallace, Phys. Rev. **71**, 622 (1974).
[7] J. C. Slonczewski and P. R. Weiss, Phys. Rev. **109**, 272 (1958).
[8] F. D. M. Haldane, Phys. Rev. Lett. **61**, 2015 (1988).
[9] A. H. Castro Neto, F. Guinea, N. M. R. Peres, K. S. Novoselov, and A. K. Geim, Rev. Mod. Phys. **81**, 109 (2009).
[10] N. M. R. Peres, A. H. Castro Neto, and F. Guinea, Phys. Rev. B. **73**, 195411 (2006).
[11] M. I. Katsnelson, K. S. Novoselov, and A. K. Geim, Nature physics **2**, 620 (2006).
[12] Andrea F. Young and Philip Kim, Nature physics **5**, 222 (2009).
[13] N. Stander, B. Huard, and D. Goldhaber-Gordon, Phys. Rev. Lett. **102**, 026807 (2009).
[14] J. Tworzydlo, B. Trauzettel, M. Titov, A. Rycerz, and C. W. J. Beenakker, Phys. Rev. Lett. **96**, 246802 (2006).
[15] R. Danneau, F. Wu, M. F. Craciun, S. Russo, M.Y. Tomi, J. Salmilehto, A. F. Morpurgo, and P. J. Hakonen, Phys. Rev. Lett. **100**, 196802 (2008).
[16] L. DiCarlo, J. R. Williams, Yiming Zhang, D. T. McClure, and C. M. Marcus, Phys. Rev. Lett. **100**, 156801 (2008).
[17] A. Rycerz, J. Tworzydl strokeo, and C. W. J. Beenakker, Nature Physics **3**, 172 (2007).
[18] Di Xiao, Wang Yao, and Qian Niu, Phys. Rev. Lett. **99**, 236809 (2007).
[19] A. R. Akhmerov, J. H. Bardarson, A. Rycerz, and C. W. J. Beenakker, Phys. Rev. B. **77**, 205416 (2008).
[20] P. San-Jose, E. Prada, E. McCann, and H. Schomerus, Phys. Rev. Lett. **102**, 247204 (2009).
[21] Fengnian Xia, Damon B. Farmer, Yu-ming Lin, and Phaedon Avouris, Nano Lett. **10**, 715 (2010).
[22] Hongki Min, Giovanni Borghi, Marco Polini, and A. H. MacDonald, Phys. Rev. B. **77**, 041407(R) (2008).
[23] M. N. Baibich, J. M. Broto, A. Fert, F. Nguyen Van Dau, F. Petroff, P. Etienne, G. Creuzet, A. Friederich, and J. Chazelas, Phys. Rev. Lett. **61**, 2472 (1988).
[24] Igor Zutic, Jaroslav Fabian, and S. Das Sarma, Rev. Mod. Phys. **76**, 323 (2004).
[25] S. Y. Zhou, G.-H. Gweon, A.V. Fedorov, P.N. First, W.A. de Heer, D.-H. Lee, F. Guinea, A. H. Castro Neto, and A. Lanzara, Nature Materials **6**, 770 (2007).
[26] Franois Varchon , R. Feng , J. Hass, X. Li, Bich N. Nguyen, Ccile Naud, Pierre Mallet, Jean Yves Veuillen , Claire Berger, E. H. Conrad, and Laurence Magaud, Phys. Rev. Lett. **99**, 126805 (2007).
[27] Gianluca Giovannetti, Pet A. Khomyakov, Geert Brocks, Paul J. Kelly, and Jeoroen Van den Brink, Phys. Rev. B **76**, 073103 (2007).
[28] Y. H. Lu, P. M. He, and Y. P. Feng, arXiv:0712.4008 (2007).
[29] I. Zanella, S. Guerini, S. B. Fagan, J. Mendes Filho, and A. G. Souza Filho, Phys. Rev. B. **77**, 073404 (2008).
[30] R. M. Ribeiro, N. M. R. Peres, J. Coutinho, and P. R. Briddon, Phys. Rev. B. **78**, 075442 (2008).
[31] D. P. Divincenzo and E. J. Mele, Phys. Rev. B. **29**, 1685 (1984).
[32] T. Ando, J. Phys. Soc. Jpn. **74**,777 (2005).
[33] R. Landauer, IBM J. Res. Dev. **1**, 223 (1957); **32**, 306 (1988).